

Homo- and mixed-valence EPR -active trinuclear manganese complexes

Dimitris P. Kessissoglou *

*Laboratory of Inorganic Chemistry, Department of Chemistry, Aristotle University of Thessaloniki,
PO Box 135, Thessaloniki 54006, Greece*

Contents

Abstract	837
1. Introduction	838
2. Homo-valence $Mn^{II}Mn^{II}Mn^{II}$ complexes	838
2.1. Open-structure trinuclear $Mn^{II}Mn^{II}Mn^{II}$ complexes	839
2.1.1. Structure	839
2.1.2. Magnetic properties	840
2.1.3. EPR study	843
2.2. Close-structure trinuclear $Mn^{II}Mn^{II}Mn^{II}$ complexes	844
3. Mixed-valence $Mn^{III}Mn^{II}Mn^{III}$ complexes	846
3.1. Open-structure mixed-valence trinuclear $Mn^{III}Mn^{II}Mn^{III}$ complexes	846
3.1.1. Structure	846
3.1.2. Magnetic properties	849
3.1.3. EPR study	851
3.2. Close-structure mixed-valence trinuclear $Mn^{III}Mn^{II}Mn^{III}$ complexes	853
Acknowledgements	856
References	856

Abstract

The chemistry of manganese has received considerable attention in recent years due to the fact that manganese is believed to be catalytically active in a variety of metalloenzymes. This

* Tel.: + 30-31-997723; fax: + 30-31-997738.

E-mail address: kessisog@chem.auth.gr (D.P. Kessissoglou)

paper deals with the study of homo- and mixed-valence EPR active trinuclear manganese complexes potential models for the polymanganese oxo centers. © 1999 Elsevier Science S.A. All rights reserved.

Keywords: Manganese; EPR active; Trinuclear; Homo-valence; Mixed-valence

1. Introduction

$4\text{H}_2\text{O} + h\nu \rightarrow 4\text{H}^+ + \text{O}_2$ is considered the most simple written and important reaction on the planet at this moment. This is because we owe our life to the oxygen released from this reaction through photosynthesis. However, 2.7 billion years ago this reaction was the most polluting factor for the environment of that day. The polluting factor was the oxygen. It was being discarded from the prokaryotes biological systems in their attempt to consume as much H_2O as possible, to use as an energy source (food). This pollutant (O_2) destroyed the atmospheric environment consisting of CO_2 and H_2 . As a result of this change, the next step of evolution started, with the creation of higher and more complicated biological systems, first plants, then animals and human beings. It has been written that human beings are the highest and most perfect biological system on the planet. I know that plants can survive without our presence, but we cannot survive without the presence of plants, having a crucial defect, that of not having chloroplasts. Coming to the chemical factors implicated in the above given reaction we can find a metal, i.e. manganese, playing a key role. It catalyzes the cleavage of water in oxygen evolving complexes (OECs). Besides that, manganese is an essential element in many other biological processes. Concerning manganese, two functional values can be distinguished; Mn^{II} as a Lewis acid and in higher oxidation states (Mn^{III} , Mn^{IV}) as an oxidative catalyst. In most Mn redox enzymes [1], Mn exists in the oxidation states $2+$, $3+$ and $4+$: Mn^{II} , in the manganese-containing ribonucleotide reductase [2–5]; a trimanganese center in inorganic pyrophosphatase [20]; a binuclear Mn^{II} site in the Mn thiosulfate oxidase [6]; a single Mn^{III} center in the manganese SOD [7] catalyzing the dismutation of superoxide radicals to oxygen and hydrogen peroxide; Mn^{III} heme center in the manganese peroxidase (MnP) [8,9] capable for the oxidative degradation of lignin; two Mn^{III} single centers in the non heme manganese catalase [10–13] and four Mn^{II} – Mn^{IV} in the OEC [14–19]. This review deals with homo- and mixed-valence open-structure trinuclear manganese complexes as potential models for the manganese containing enzymes, while for the analogous close-structure complexes only the structural characteristics are discussed.

2. Homo-valence $\text{Mn}^{\text{n}}\text{Mn}^{\text{n}}\text{Mn}^{\text{n}}$ complexes

These complexes may be used as models for the following metalloproteins: concanavalin A, the reduced form of ribonucleotide reductase, the trimanganese center in inorganic pyrophosphatase and the manganese center of the OEC.

2.1. Open-structure trinuclear $Mn^{II}Mn^{II}Mn^{II}$ complexes

2.1.1. Structure

The first example of the synthesis and characterization of divalent linear trinuclear complexes with the formula $Mn^{II}Mn^{II}Mn^{II}(OAc)_6(biphme)_2$ appeared in 1990 [21,22]. These are comprised of a linear array of three Mn^{II} ions in which a central hexacoordinate Mn^{II} ion that resides on a crystallographic inversion center in the *anti*-isomers is flanked by two metal ions that are essentially pentacoordinate. The metals are bridged by four bidentate and two monodentate μ -acetato ligands. The reaction used to prepare these trinuclear complexes is not restricted to biphme. Other bidentate, nitrogen-donating ligands may be employed, as evidenced by the synthesis of $Mn^{II}Mn^{II}Mn^{II}(OAc)_6(phen)_2$, $Mn^{II}Mn^{II}Mn^{II}(O_2CPh)_6(bpy)_2$, $Mn^{II}Mn^{II}Mn^{II}(OAc)_6(bpy)_2$, $Mn^{II}Mn^{II}Mn^{II}(OAc)_2(bpc)_2(py)_4(H_2O)_2$ and $Mn^{II}Mn^{II}Mn^{II}(AcO)_6(pybim)_2$ [21–24] (Table 1).

All the trinuclear $Mn^{II}Mn^{II}Mn^{II}$ complexes reported thus far obey the ‘carboxylate shift’ model described by Lippard et al. [21]. According to this model, there is a linear correlation between $Mn_{int} \cdots O_d$, D, and $Mn_{int} \cdots O_b$, B (Fig. 1).

Thus, as D decreases, B lengthens, ultimately leading to a shift in the monodentate bridging carboxylate ligand to a bidentate bridging mode, a behavior also observed in the $Mn(II)$ ribonucleotide reductase protein R2 and in the reduced R2 [4,5].

More specifically, the complex $Mn^{II}Mn^{II}Mn^{II}(AcO)_6(pybim)_2$ consists of a linear array of divalent manganese ions (Fig. 2). The central Mn^{II} , which is located on a crystallographic inversion center, is coordinated octahedrally by six acetate oxygen atoms. The central Mn^{II} and the terminal Mn^{II} atoms are bridged by four acetate ligands in bidentate fashion, whereas the other two acetate groups form bridges in the monodentate mode. The two terminal Mn^{II} ions are five coordinated with the pybim molecule acting as bidentate capping ligand. The free oxygen atoms of the monodentate acetates interact weakly with the terminal $Mn(II)$ atoms [$O(5) \cdots Mn(2)$ 2.823 Å] and block the sixth coordination site of the terminal metal ion.

Table 1
Open-structure trinuclear $Mn^{II}Mn^{II}Mn^{II}$ complexes^a

Formula	$Mn \cdots Mn$ (Å)	μ_{eff}	J (cm^{-1})	S	Ref.
<i>anti</i> - $Mn^{II}Mn^{II}Mn^{II}(OAc)_6(biphme)_2$	3.700	9.85	−1.8	5/2	[21]
<i>anti</i> - $Mn^{II}Mn^{II}Mn^{II}(OAc)_6(biphme)_2$	3.635	9.85	−2.8	5/2	[23]
<i>syn</i> - $Mn^{II}Mn^{II}Mn^{II}(OAc)_6(biphme)_2$	3.560	9.85	−2.8	5/2	[21,23]
$Mn^{II}Mn^{II}Mn^{II}(OAc)_6(phen)_2$	3.387	—	—	—	[23]
$Mn^{II}Mn^{II}Mn^{II}(O_2CPh)_6(bpy)_2$	3.588	—	—	—	[23]
$Mn^{II}Mn^{II}Mn^{II}(OAc)_6(bpy)_2$	3.614	9.75	−4.4	5/2	[22]
$Mn^{II}Mn^{II}Mn^{II}(OAc)_2(bpc)_2(py)_4(H_2O)_2$	3.289	9.79	−1.43	5/2	27b
$Mn^{II}Mn^{II}Mn^{II}(AcO)_6(pybim)_2$	3.558	9.4	−1.9	5/2	[24]

^a biphme = methoxy-bis(1-methylimidazol-2-yl)phenylmethane; phen = 1,10 phenanthroline; bpy = 2,2′-bipyridine; H_2bpc = 2,2′-bipyridyl-3,3′-dicarboxylic acid; pybim = 2-(2-pyridyl)benzimidazol.

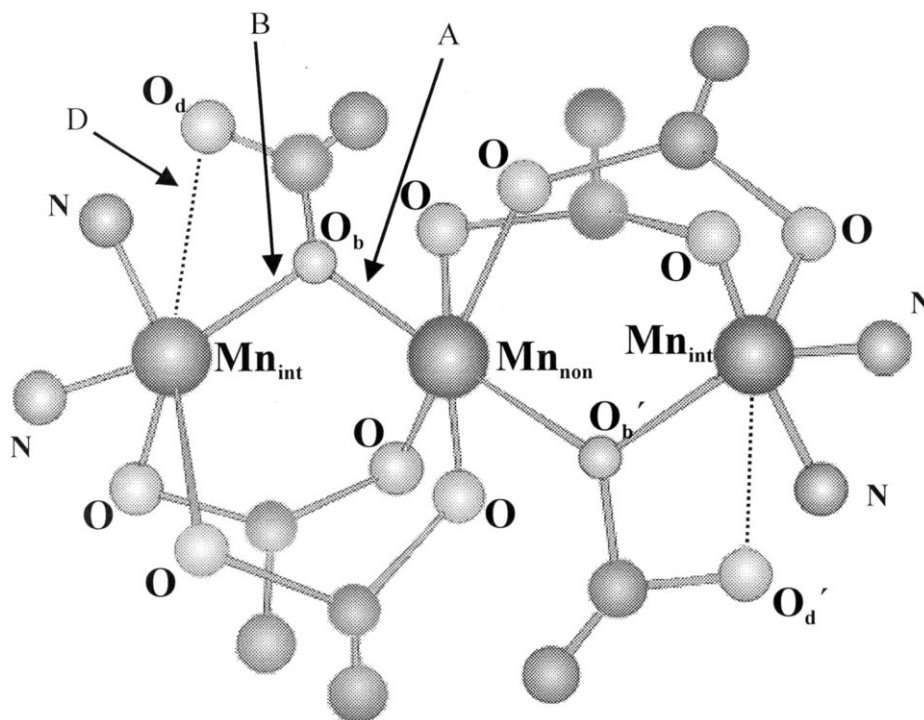


Fig. 1. A general scheme of $\text{Mn}^{\text{II}}\text{Mn}^{\text{II}}\text{Mn}^{\text{II}}$ trinuclear complexes, showing the dangling (O_d) and the bridging (O_b) oxygen atoms of the monodentate carboxylates, the central metal, Mn_{non} , which does not interact with O_d .

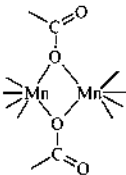
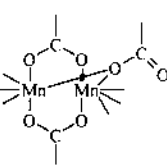
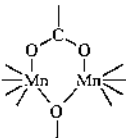
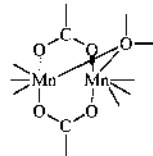
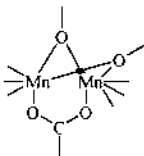
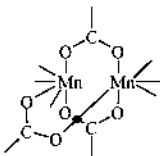
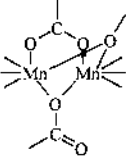
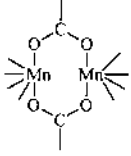
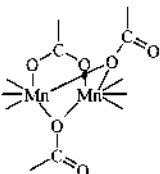
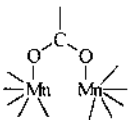
The coordination geometry around Mn^{II} is square pyramidal with severe trigonal distortion as indicated by the trigonality index $\tau = (164.17 - 131.69)/60 = 0.54$. The $\text{O}(5) \cdots \text{Mn}(2)$ distance of 2.823 Å is the longest for a series of analogous compounds and the $\text{Mn}(2) - \text{O}(6)$ distance of 2.132(2) Å the shortest. Considering the $\text{Mn} \cdots \text{Mn}$ separation, it depends on the coordination mode and the number of carboxylate bridging ligands (Table 2). The carboxylate ligands act in unidentate or bidentate bridging modes while the number of the carboxylato groups varies between one and three. The $\text{Mn} \cdots \text{Mn}$ separations observed for this type of tricarboxylate-bridged units can accommodate a considerable degree of flexibility (3.37–3.71 Å).

2.1.2. Magnetic properties

All the homo-valence Mn^{II} trinuclear compounds studied until now show a weak antiferromagnetic coupling with J coupling varying from -1.8 to -4.4 cm^{-1} (Table 1). For $\text{Mn}^{\text{II}}\text{Mn}^{\text{II}}\text{Mn}^{\text{II}}(\text{AcO})_6(\text{pybim})_2$ the molar magnetic susceptibility and the $\mu_{\text{eff}}/3\text{Mn}$ vs. T are shown in Fig. 3.

Table 2

Mn^{II}...Mn^{II} separation with various coordination modes of the carboxylato bridges*

Coordination mode	Mn ^{II} ...Mn ^{II} separation (Å)	Coordination mode	Mn ^{II} ...Mn ^{II} separation (Å)
1 	3.53 ^a	6 	3.387 ^d , 3.614 ^e , 3.635 ^f , 3.700 ^f , 3.658 ^f , 3.560 ^f , 3.716 ^f , 3.691 ^f , 3.370 ^f , 3.600 ^g , 3.753 ^h
2 	3.760 ^g	7 	3.29 ⁱ , 3.50 ⁱ , 3.351 ^k , 3.595 ^v , 3.621 ^v , 3.589 ^u
3 	3.150 ^x , 3.163 ^y	8 	4.034 ^l , 4.558 ^m , 4.444 ⁿ
4 	3.35 ^b	9 	4.145 ^o , 4.643 ^p , 4.849 ^t , 4.557 ^t
5 	3.289 ^c	10 	5.40 ^q , 5.45 ^s , 5.598 ^r , 5.7 ^g & 6.4 ^g

* Footnotes: ^aMn[C₆H₂Cl₃OCH₂COO]₂(H₂O)₄ [25]; ^bMn(C₂H₅COO)₂(H₂O)₂ [26]; ^cMn₃(CH₃COO)₂(bpc)₂(py)₄(H₂O)₂ [27b]; ^dMn₃(CH₃COO)₆(phen)₂ [23]; ^eMn₃(CH₃COO)₆(bpy)₂ [22]; ^fMn₃(CH₃COO)₆(biphe)₂ [23]; ^gMn(CH₃COO)₂ · 4H₂O [28]; ^hMn{HB(3,5-Prⁱp₂)₃}(μ-OBz)₃Mn(3,5-Prⁱp₂H)₂, (HB(3,5-Prⁱp₂)₃ = hydrotris(3,5-diisopropyl-1-pyrazolyl)borate, 3,5-Prⁱp₂H = 3,5-diisopropylpyrazole, OBz = benzoate) [29]; ⁱK₂{Mn(H₂O)₂[Mn₃O(HCOO)₉]₂} [30]; ^j[L₂Mn₂(μ-OH)(μ-CH₃COO)₂](ClO₄) (L = N,N',N''-trimethyl-1,4,7-triazacyclononane) [31]; ^k[L₂Mn₂(μ-OH)(μ-MeCOO)₂](PF₆) (L = N,N',N''-trimethyl-1,4,7-triazacyclononane) [32]; ^l[L₂Mn(μ-CH₃COO)₃](BPh₄) (L = N,N',N''-trimethyl-1,4,7-triazacyclononane) [31]; ^m[Mn{(CH₃)₃NCH₂COO}₃]_n · nMnCl₄ [33]; ⁿMn₃(CF₃COO)₆(benz)₆ (benz = benzonitrile) [27a]; ^o[Mn(tpa)(μ-MeCOO)]₂(TCNQ)₂, (tpa = tris(2-pyridylmethyl)amine, TCNQ = tetracyanoquinodimethane) [34]; ^p[Mn₂(bpy)₄(ta)](ClO₄)₂ (ta = terephthalate) [35]; ^q[Mn[C₆H₃(CH₃)ClOCH₂COO]₂(H₂O)₂]_n [36]; ^r[{Mn(bpy)₂(H₂O)₂}{(CH₃)₃NCH₂COO}](ClO₄)₄ · 2H₂O [37]; ^s[Mn(C₄H₄O₅)(H₂O)]_n · H₂O [38]; ^tMn₂(XDK)(NO₃)(CH₃OH)₄(H₂O) and Mn₂(XDK)(bpy)₂(NO₃)(H₂O), H₂XDK = *m*-Xylenediaminebis (Kemp's triacid imide) [39]; ^uMn₂(LO)(μ-OAc)₂(ClO₄) (LOH = 2,6-bis(2-(2-pyridyl)ethyl)aminomethylphenol) [40]; ^v[Mn₂(H₂O)(piv)₄(Mepy)₂] and Mn₂(H₂O)(OAc)₄(tmeda)₂ (piv = pivalate, Me₂bpy = 4,4'-dimethyl-2,2'-bipyridine, tmeda = N,N',N''-tetramethylethylenediamine) [41]; ^yMn₃(py)₅(OAc)₃(μ₃-OH)(cat) [42].

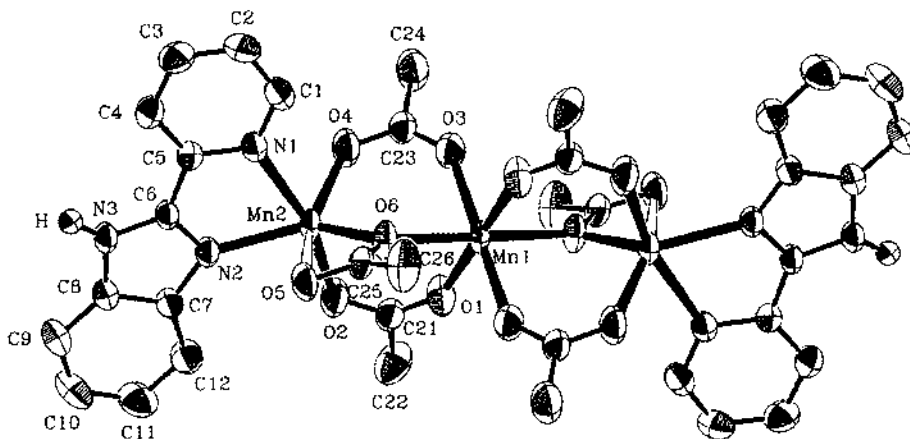


Fig. 2. ORTEP view of $\text{Mn}^{\text{II}}\text{Mn}^{\text{II}}\text{Mn}^{\text{II}}(\text{AcO})_6(\text{pybim})_2$ with 50% thermal ellipsoids showing the atom labeling scheme.

Examination of the temperature-dependence of the $\mu_{\text{eff}}/3\text{Mn}$ reveals that at room temperature (r.t.) its value is $9.4 \mu_{\text{B}}$ and decreases to $5.16 \mu_{\text{B}}$ at 4 K. This decrease from $5.43 \mu_{\text{B}}/\text{Mn}$ to $3.0 \mu_{\text{B}}/\text{Mn}$ is indicative of a small antiferromagnetic interac-

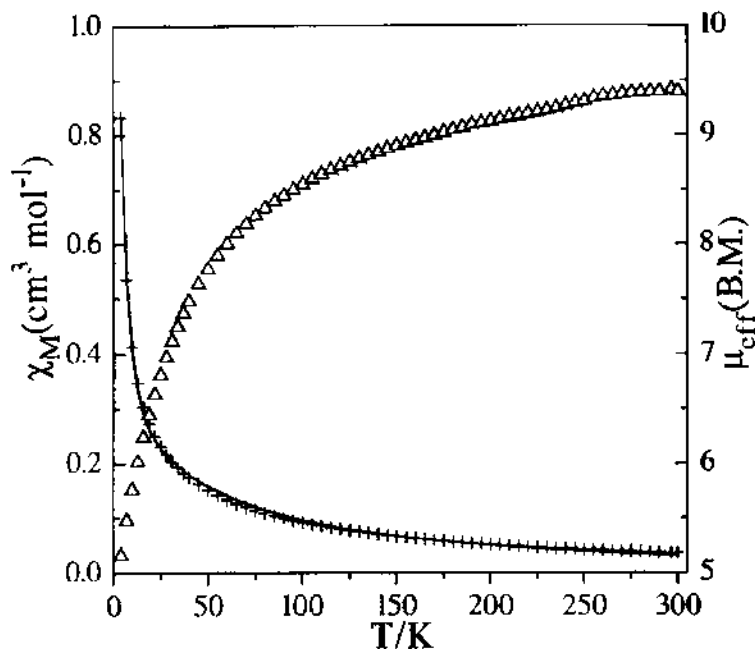


Fig. 3. Variation of χ_{M} and μ_{eff} with temperature of $\text{Mn}^{\text{II}}\text{Mn}^{\text{II}}\text{Mn}^{\text{II}}(\text{AcO})_6(\text{pybim})_2$.

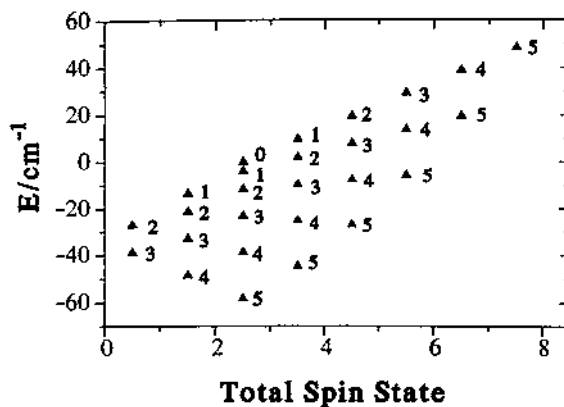


Fig. 4. Spin levels for $\text{Mn}^{\text{II}}\text{Mn}^{\text{II}}\text{Mn}^{\text{II}}(\text{AcO})_6(\text{pybim})_2$. The energy (in cm^{-1}) is given as a function of the spin value. To the right of the levels, the S_{13} values are given.

tion. The isotropic Heisenberg Hamiltonian, assuming that the interaction between the terminal Mn^{II} ions is negligible at 7.116 Å, is as follows:

$$H = -2J_1(S_1S_2 + S_2S_3) + H_{\text{Zeeman}} \quad (1)$$

where $S_1 = S_2 = S_3 = 5/2$ and the Zeeman term is given by Eq. (2):

$$H_{\text{Zeeman}} = g\mu_B(S_1 + S_2 + S_3)B \quad (2)$$

According to the standard vector coupling rules, the energy values are obtained as follows:

$$E(S, S_{13}) = -J_1[S_T(S_T + 1) - S_{13}(S_{13} + 1) - 35/4] \quad (3)$$

where S_T assumes values $S_{13} + S_2 \dots S_{13} - S_2$ and S_{13} assumes values $S_1 + S_3 \dots S_1 - S_3$. The obtained parameters are $J_1 = -1.9 \text{ cm}^{-1}$, $g = 2.02$ and $zJ = -0.1 \text{ cm}^{-1}$.

The energy scheme of this compound is shown in Fig. 4 and the ground state is $|S_2 = 5/2, S_{13} = 5, S = 5/2\rangle$, having the first excited $|S_2 = 5/2, S_{13} = 4, S = 3/2\rangle$ at $5|J|$ and the second $|S_2 = 5/2, S_{13} = 5, S = 7/2\rangle$ at $7|J|$.

2.1.3. EPR study

EPR studies have been reported only for the $\text{Mn}^{\text{II}}\text{Mn}^{\text{II}}\text{Mn}^{\text{II}}(\text{OAc})_6(\text{bpy})_2$ and the $\text{Mn}^{\text{II}}\text{Mn}^{\text{II}}\text{Mn}^{\text{II}}(\text{AcO})_6(\text{pybim})_2$ compounds. For both complexes the EPR spectra exhibit a broad signal centered at $g = 2.0$ with weak features at $g = 6.3, 3.0, 2.05, 1.7, 1.04$ and $g = 4.5, 6.5$, respectively. The temperature-dependence of the intensity of the signal at $g = 2.0$ for $\text{Mn}^{\text{II}}\text{Mn}^{\text{II}}\text{Mn}^{\text{II}}(\text{AcO})_6(\text{pybim})_2$ is shown in Fig. 5. The intensity of the signal was calculated by integration of the magnetic field in the range 2000–5000 G. It decreases continuously from 8 to 60 K, while for the

temperature range 4–8 K the signal shows a small increase with a maximum intensity of around 8.0 K. The small decrease at temperatures lower than 8.0 K is probably due to antiferromagnetic intermolecular interactions. The magnitude of the antiferromagnetic interaction is further confirmed by the small but steady increase of the linewidth upon cooling, which is evidence of a small interaction.

2.2. Close-structure trinuclear $Mn^{II}Mn^{II}Mn^{II}$ complexes

While the chemistry of the oxo-centered equilateral triangle of the basic carboxylates with numerous of metal ions has been well established [43], only recently the crystal structure of a homo-valence $Mn(II)$ complex has been reported [42].

$Mn^{II}Mn^{II}Mn^{II}(AcO)_3(\mu_3-OH)(cat)(py)_5$ has a pyramidal $Mn^{II}Mn^{II}Mn^{II}(\mu_3-OH)$ unit with three acetate ligands spanning the edges of a $(Mn^{II})_3$ isosceles triangle. The asymmetry of the pyramidal $Mn^{II}Mn^{II}Mn^{II}(\mu_3-OH)$ unit is apparent in the unequal $Mn\cdots Mn$ distances (3.150, 3.163, 3.760 Å) and $Mn-OH-Mn$ angles (92.0, 92.0, 119.0°). It shows intratrimer antiferromagnetic interaction with J and J_{13} values of -2.36 and -1.92 cm^{-1} , respectively (Table 3).

Trinuclear $Mn^{III}Mn^{III}Mn^{III}$ complexes possess the 'basic carboxylate' structure having the Mn_3O core. The structure is similar to that observed for the mixed-valence $Mn^{III}Mn^{II}Mn^{III}$ complexes and is described in more detail below.

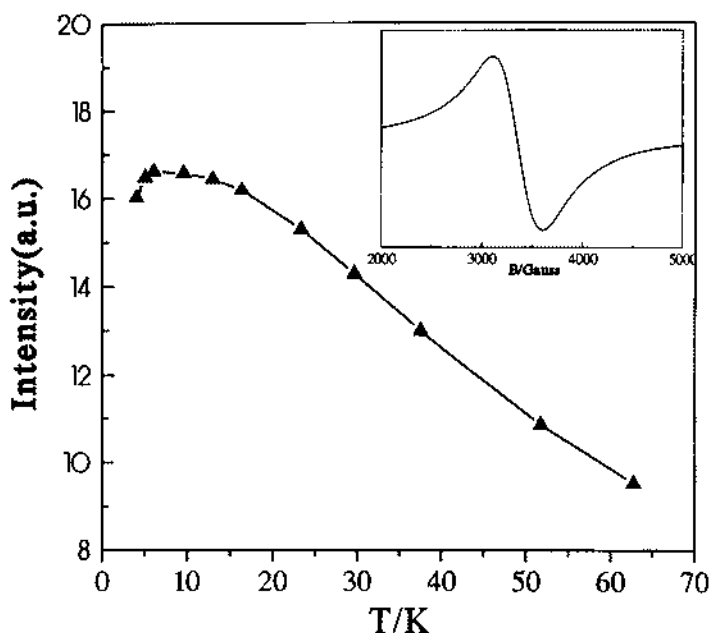


Fig. 5. Temperature dependence of the intensity of the signal $g = 2$ (inset) over the field range 2000–4500 G for $Mn^{II}Mn^{II}Mn^{II}(AcO)_6(pybim)_2$.

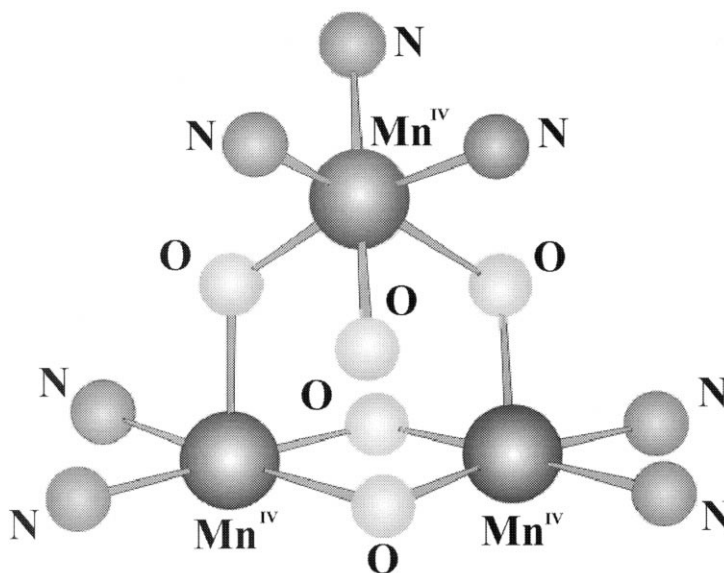
Table 3

Close-structure trinuclear $\text{Mn}^n\text{Mn}^n\text{Mn}^n$ complexes^a

Formula	Mn...Mn (Å)	μ_{eff}	J (cm^{-1})	J' (cm^{-1})	S	Ref.
$\text{Mn}^{\text{II}}\text{Mn}^{\text{II}}\text{Mn}^{\text{II}}(\text{AcO})_3(\mu_3\text{-OH})(\text{cat})(\text{py})_5$	3.150, 3.163, 3.760	—	−2.36	—	—	[43]
$[\text{Mn}^{\text{III}}\text{Mn}^{\text{III}}\text{Mn}^{\text{III}}\text{O}(\text{OAc})_6(\text{py})_3]\text{ClO}_4$	—	4.25	−10.2	—	0	[83]
$\text{K}_2\{\text{Mn}(\text{H}_2\text{O})_2[\text{Mn}_3\text{O}(\text{HCOO})_9]_2$	3.29	13.0	—	—	—	[30]
$\text{Mn}^{\text{IV}}\text{Mn}^{\text{IV}}\text{Mn}^{\text{IV}}\text{O}_4(\text{OH})(\text{bpea})_3(\text{ClO}_4)_3$	—	4.53	−76	−11	3/2	[77]
$[\{\text{Mn}^{\text{IV}}\text{Mn}^{\text{IV}}\text{Mn}^{\text{IV}}\text{O}_4(\text{OH})(\text{tpen})_3\}_2(\mu\text{-tpen})](\text{ClO}_4)_6$	2.625, 3.192	—	—	—	3/2	[78]
$\text{Mn}^{\text{IV}}\text{Mn}^{\text{IV}}\text{Mn}^{\text{IV}}\text{O}_4(\text{phen})_3(\text{H}_2\text{O})_2(\text{NO}_3)_4$	2.675, 3.249	3.75	—	—	—	[79]
$\text{Mn}^{\text{IV}}\text{Mn}^{\text{IV}}\text{Mn}^{\text{IV}}\text{O}_4(\text{bpy})_4(\text{H}_2\text{O})_2(\text{ClO}_4)_4$	2.679, 3.246, 3.263	4.60	−182	−98	1/2	[80]
$\text{Mn}^{\text{IV}}\text{Mn}^{\text{IV}}\text{Mn}^{\text{IV}}\text{O}_4(\text{bpy})_4\text{Cl}_2[\text{CdCl}_4]$	2.681, 3.241, 3.245	3.79	−171	−108	1/2	[81]

^a H_2cat = catecholate; bpea = N,N -bis(2-pyridylmethyl)ethyamine; tpen = N,N,N',N' -tetrakis(2-pyridylmethyl)-1,2-ethanediamine).

$\text{Mn}^{\text{IV}}\text{Mn}^{\text{IV}}\text{Mn}^{\text{IV}}$ complexes have a Mn_3O_4 core (Fig. 6). The three manganese atoms occupy the vertices of a triangle. One of the manganese atoms is linked to the other two manganese atoms by means of two individual μ -oxo bridges while the other two are linked to each other by two mutual μ -oxo bridges. The distances

Fig. 6. The Mn_3O_4 core of the $\text{Mn}^{\text{IV}}\text{Mn}^{\text{IV}}\text{Mn}^{\text{IV}}$ complexes.

between the single-bridged Mn atoms vary from 3.192 to 3.263 Å and are considerably longer than the doubly-bridged Mn atoms which vary from 2.625 to 2.681 Å [77–80].

3. Mixed-valence $\text{Mn}^{\text{III}}\text{Mn}^{\text{II}}\text{Mn}^{\text{III}}$ complexes

Mixed-valence $\text{Mn}^{\text{III}}\text{Mn}^{\text{II}}\text{Mn}^{\text{III}}$ complexes may be used as models for the reaction center of the OEC. The available data strongly suggests that a polynuclear cluster is responsible for the EPR detectable signals in the ‘active form’ [44,45] of S_1 ($g = 4.8$ in parallel polarization) and S_2 ($g = 2$ multiline and $g = 4.1$ with fine structure) oxidation states of the OEC [46–50], while a multiline signal for the So^* state has been reported recently [51]. In addition, EXAFS data [1,16,52–54] indicate the presence of at least two ~ 2.7 Å Mn···Mn interactions, in addition to an interaction at ~ 3.3 Å. The 2.7 Å distances correspond to high-valent $\text{Mn}_2(\mu\text{-O})_2$ units, which have been shown to have similar Mn–Mn distances. X-ray absorption near-edge structure (XANES) measurements [52–57] suggest 3.0–3.5 and 3.25–3.75 average oxidation states per manganese in the lower S states. Based on these data a, number of structural proposals were addressed (dimer of dimers, trimer/monomer, distorted cubane, butterfly, dimer/monomer).

3.1. Open-structure mixed-valence trinuclear $\text{Mn}^{\text{III}}\text{Mn}^{\text{II}}\text{Mn}^{\text{III}}$ complexes

3.1.1. Structure

The first open-structure $\text{Mn}^{\text{III}}\text{Mn}^{\text{II}}\text{Mn}^{\text{III}}$ complex reported was $\alpha\text{-Mn}^{\text{III}}\text{Mn}^{\text{II}}\text{Mn}^{\text{III}}(\text{Hsaladhp})_2(\text{OAc})_4(\text{CH}_3\text{OH})_2$ [58]. After that, a series of mixed-valence compounds of the general composition $\text{Mn}^{\text{III}}\text{Mn}^{\text{II}}\text{Mn}^{\text{III}}(\text{X-Hsaladhp})_2(\text{AcO})_4(\text{CH}_3\text{OH})_2$ were prepared by adding the Schiff-base ligand to $\text{Mn}(\text{AcO})_2 \cdot 4\text{H}_2\text{O}$ or $\text{Mn}(\text{AcO})_3$ in methanol and air [59,60]. These trimers react with X-salicylic acid ($\text{X} = \text{Cl}, \text{Br}$) in methanol, dmf or thf to yield mixed acetato/salicylato trinuclear complexes which have been isolated as dark brown solids [24,61] (Table 4).

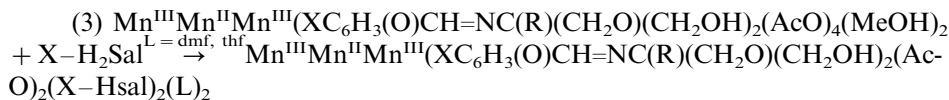
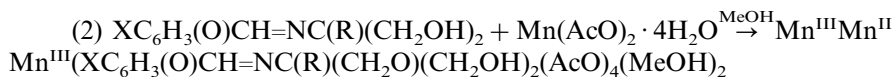
The reaction can take place in all of those solvents, leading to the formation of trinuclear compounds in contrast to the preparation of the trinuclear complexes with only acetates as bridging ligands in which in the presence of dmf, mononuclear Mn^{IV} complexes [62,63] and MnO_2 are formed exclusively. Using MnCl_2 as starting material, $\text{Mn}^{\text{III}}\text{Mn}^{\text{II}}\text{Mn}^{\text{III}}(5\text{-Cl-Hsaladhp})_2(\text{Hsal})_4$ has been isolated. To obtain the trinuclear compounds it is absolutely essential not to add an additional strong base, such as sodium methoxide or sodium hydroxide, which lead to mononuclear Mn^{IV} complexes. In the presence of CH_3CN , a polymeric compound [61] with the same trimeric unit but significant deviation from linearity $\text{Mn}^{\text{III}}\text{--Mn}^{\text{II}}\text{--Mn}^{\text{III}} = 137.5^\circ$ has been isolated and structurally characterized. Generally, nitrogen-donor solvents (e.g. CH_3CN , py, en) are not bound at the sixth position of Mn^{III} ion. The reactions involve deprotonation of the ligand without using a base as follows:

Table 4

Open-structure trinuclear $\text{Mn}^{\text{III}}\text{Mn}^{\text{II}}\text{Mn}^{\text{III}}$ complexes^a

Formula	Mn...Mn (Å)	J (cm^{-1})	g_1	Ref.
$\alpha\text{-Mn}^{\text{III}}\text{Mn}^{\text{II}}\text{Mn}^{\text{III}}(\text{Hsaladh})_2(\text{OAc})_4(\text{CH}_3\text{OH})_2$	3.551	−7.1	2.01	[58]
$\alpha\text{-Mn}^{\text{III}}\text{Mn}^{\text{II}}\text{Mn}^{\text{III}}(5\text{-Cl-Hsaladh})_2(\text{OAc})_4(\text{CH}_3\text{OH})_2$	3.511	—	—	[24]
$\beta\text{-Mn}^{\text{III}}\text{Mn}^{\text{II}}\text{Mn}^{\text{III}}(\text{Hsaladh})_2(\text{OAc})_4(\text{CH}_3\text{OH})_2$	3.502	−6.7	2.01	[59]
$\alpha\text{-Mn}^{\text{III}}\text{Mn}^{\text{II}}\text{Mn}^{\text{III}}(\text{Hsaladh})_2(\text{OAc})_4(\text{H}_2\text{O})_2$	3.419	−7.1	2.08	[60]
$\alpha\text{-Mn}^{\text{III}}\text{Mn}^{\text{II}}\text{Mn}^{\text{III}}(\text{Hsaladh})_2(\text{OAc})_4(\text{pyOH})_2$	3.484	−5.3	2.10	[60]
$\alpha\text{-Mn}^{\text{III}}\text{Mn}^{\text{II}}\text{Mn}^{\text{III}}(\text{Hsalathm})_2(\text{OAc})_4(\text{CH}_3\text{OH})_2$	3.515	−5.9	2.03	[60]
$\alpha\text{-Mn}^{\text{III}}\text{Mn}^{\text{II}}\text{Mn}^{\text{III}}(\text{Hsaladh})_2(\text{OAc})_2(5\text{-Cl-Hsal})_2(\text{thf})_2$	3.507	−5.6	1.95	[24]
$\alpha\text{-Mn}^{\text{III}}\text{Mn}^{\text{II}}\text{Mn}^{\text{III}}(\text{Hsaladh})_2(\text{OAc})_2(\text{Hsal})_2(\text{dmf})_2$	3.510	—	—	[64]
$[\beta\text{-Mn}^{\text{III}}\text{Mn}^{\text{II}}\text{Mn}^{\text{III}}(\text{Hsaladh})_2(\text{OAc})_2(5\text{-Cl-Hsal})_2]_n$	3.417	−5.5	1.95	[61]
$\text{Mn}^{\text{III}}\text{Mn}^{\text{II}}\text{Mn}^{\text{III}}(5\text{-Cl-Hsaladh})_2(\text{Hsal})_4$	3.495	−5.7	2.02	[65]
$\text{Mn}^{\text{III}}\text{Mn}^{\text{II}}\text{Mn}^{\text{III}}(\text{L}^1)_2(\text{mcba})(\text{OCH}_3)_2$	3.172	—	—	[66]
$\text{Mn}^{\text{III}}\text{Mn}^{\text{II}}\text{Mn}^{\text{III}}(\text{L}^2)_2(\text{mcba})(\text{OCH}_3)_2$	3.172	1.9	2.06	[66]
$\text{Mn}^{\text{III}}\text{Mn}^{\text{II}}\text{Mn}^{\text{III}}(\text{L}^1)_2(\text{bf})(\text{OCH}_3)_2$	3.154, 3.137	—	—	[66]
$\text{Mn}^{\text{III}}\text{Mn}^{\text{II}}\text{Mn}^{\text{III}}(\text{L}^2)_2(\text{ba})(\text{OCH}_3)_2$	—	1.9	2.00	[66]
$\text{Mn}^{\text{III}}\text{Mn}^{\text{II}}\text{Mn}^{\text{III}}(\text{L}^1)_2(\text{ba})(\text{OCH}_3)_2$	—	1.05	1.98	[66]
$\text{Mn}^{\text{III}}\text{Mn}^{\text{II}}\text{Mn}^{\text{III}}(3,5\text{-}t\text{-Bu}_2\text{C}_6\text{H}_2\text{O}_2)_4(\text{py})_4$	3.136, 3.162	—	—	[67]
$[\text{Mn}^{\text{III}}\text{Mn}^{\text{II}}\text{Mn}^{\text{III}}(\text{malonate})_4(\text{H}_2\text{O})_6]_n$	5.215	—	—	[68]
$[\text{Mn}^{\text{II}}\text{Mn}^{\text{III}}\text{Mn}^{\text{II}}(\text{sal})_2(\text{Hsal})_2(\text{H}_2\text{O})_4(4\text{-Me-py})_6]^+$	5.016	−0.53	—	[69]
$[\text{Mn}^{\text{II}}\text{Mn}^{\text{III}}\text{Mn}^{\text{II}}(\text{L-rha})_2(\text{H}_2\text{O})]\text{NO}_3$	3.845	—	—	[70]
$[\text{Mn}^{\text{II}}\text{Mn}^{\text{III}}\text{Mn}^{\text{II}}(\text{D-man})_2(\text{H}_2\text{O})]\text{Cl}$	3.911	Antiferr	—	[70]
$[\text{Mn}^{\text{VI}}\text{Mn}^{\text{V}}\text{Mn}^{\text{VI}}(\text{NBu}^t)_4(\text{i-NBu}^t)_4]^+$	2.463–2.490	—	—	[71]

^a $\text{H}_2\text{L}^1 = N\text{-(2-hydroxybenzyl)}\text{-}N\text{-(2-hydroxybenzyl)}\text{-}N',N''\text{-dimethylethylenediamine}$; $\text{H}_2\text{L}^2 = N\text{-(3,5-di-}t\text{-butyl-2-hydroxybenzyl)}\text{-}N\text{-(2-hydroxybenzyl)}\text{-}N',N''\text{-dimethylethylenediamine}$; $\text{Hmcba} = m\text{-chlorobenzoic acid}$; $\text{Hbf} = \text{benzoylformic acid}$; $\text{Hba} = \text{benzoic acid}$; $\text{H}_3\text{saladh} = 1,3\text{-dihydroxy-2-methyl-(salicylideneamino)propane}$; $5\text{-Cl-H}_3\text{saladh} = 1,3\text{-dihydroxy-2-methyl-(5-Cl-salicylidene-amino)propane}$; $\text{HOAc} = \text{acetic acid}$; $\text{H}_2\text{sal} = \text{salicylic acid}$; $5\text{-Cl-H}_2\text{sal} = 5\text{-chloro-salicylic acid}$; $\text{dmf} = \text{dimethylformamide}$; $\text{thf} = \text{tetrahydrofuran}$; $\text{Hsalathm} = \text{tris(hydroxymethyl)(salicylideneamino)methane}$; $\text{D-man} = \text{tris}[(N\text{-D-mannose})\text{aminoethyl}]\text{amine}$; $\text{L-rha} = \text{tris}[(N\text{-6-deoxy-L-mannose})\text{aminoethyl}]\text{amine}$.



The following description of the complex $\text{Mn}^{\text{III}}\text{Mn}^{\text{II}}\text{Mn}^{\text{III}}(\text{Hsaladh})_2(\text{AcO})_2(5\text{-Cl-Hsal})_2(\text{thf})_2$ shown in Fig. 7 could be considered as a representative structural description of the series of the linear mixed-valence $\text{Mn}^{\text{III}}\text{Mn}^{\text{II}}\text{Mn}^{\text{III}}$ trinuclear compounds characterized as α -isomers, in contrast to the bent arrangement of the manganese atoms which have been characterized as β -isomers (Table 4).

The complex includes a central, octahedral Mn^{II} ion $\text{Mn}(1)$ that is located on a crystallographic inversion center. It is flanked by two tetragonally-distorted Mn^{III} ions $\text{Mn}(2)$. The coordination octahedral environment of central Mn^{II} is composed of two *syn*-bridging acetates and salicylates and two μ -alkoxo oxygen atoms of the Schiff base ligand. Each Mn^{III} is six coordinate using an acetate, a salicylate, a tridentate Schiff base ligand and a neutral axial oxygen-donor ligand. The neutral unidentate ligand occupies the Jahn–Teller distorted axes along with the salicylato oxygen [O(9) and O(6)]. The elongation is shown by a comparison of $\text{Mn}(2)–\text{N}(1) = 1.991(3)$ Å and $\text{Mn}(2)–\text{O}(4) = 1.951(3)$ Å, the longest distances on the meridional plane and the axial distances $\text{Mn}(2)–\text{O}(6) = 2.174(3)$ Å and $\text{Mn}(2)–\text{O}(9) = 2.405(3)$ Å. The $\text{H}_3\text{saladhp}$ ligand acts as a tridentate chelating agent by using an imine nitrogen, and phenolate and alkoxide oxygen atoms to coordinate to Mn^{III} . The central $\text{Mn}(1)$ and the terminal $\text{Mn}(2)$ ions are bridged by the alkoxide oxygen from the $\text{H}_3\text{saladhp}$ ligand, an acetato, and a carboxylato oxygen from the 5-Cl-salicylato ligand resulting in a $3.507(1)$ Å $\text{Mn}(1)\cdots\text{Mn}(2)$ separation with a $120.95(10)^\circ$ $\text{Mn}(1)–\text{O}(\text{alkoxide})–\text{Mn}(2)$ angle. The acetato oxygen lies on the meridional plane with a distance of $\text{Mn}(2)–\text{O}(4) = 1.951(3)$ Å, while the salicylato oxygen occupies the axial position of the octahedron with a distance of $\text{Mn}(2)–\text{O}(6) = 2.174(3)$ Å. The cluster is valence trapped, as evidenced by the long central Mn^{II} to heteroatom bond lengths and by Jahn–Teller distortion of the terminal high spin Mn^{III} ions.

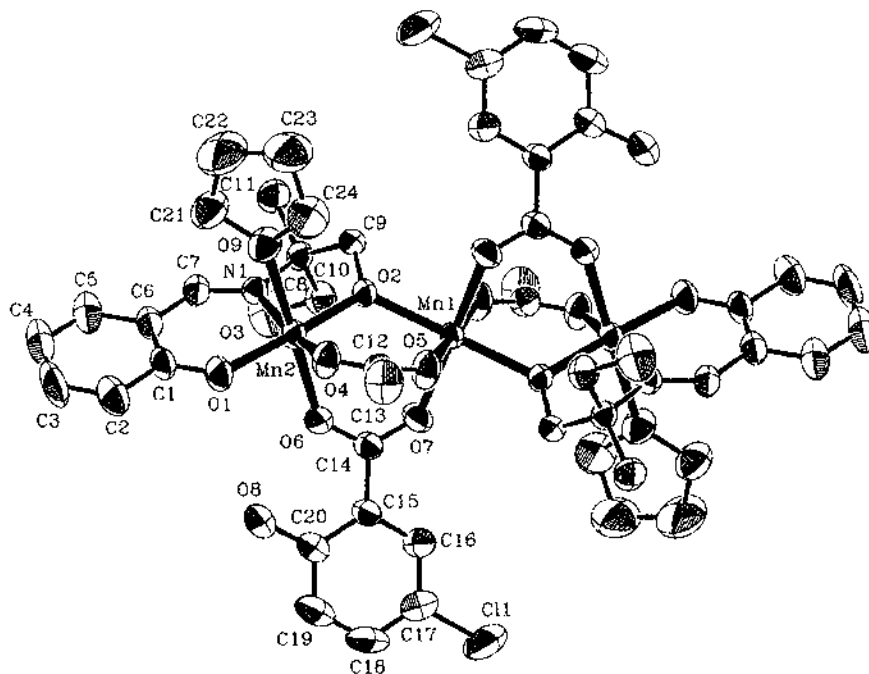


Fig. 7. ORTEP view of $\text{Mn}^{\text{III}}\text{Mn}^{\text{II}}\text{Mn}^{\text{III}}(\text{Hsaladhp})_2(\text{AcO})_2(5\text{-Cl-Hsal})_2(\text{thf})_2$ with 50% thermal ellipsoids showing the atom labeling scheme.

Recently, some very interesting mixed-valence trinuclear complexes with oxidation states II/III/II and VI/V/VI have been reported [70,71].

$[\text{Mn}^{\text{III}}\text{Mn}^{\text{II}}\text{Mn}^{\text{III}}(\text{L-rha})_2(\text{H}_2\text{O})]\text{NO}_3$ has a linear-ordered trimanganese core bridged by two carbohydrates residues with a $\text{Mn}\cdots\text{Mn}$ separation of 3.845 Å. The terminal Mn^{II} atoms are seven-coordinate with a distorted mono-faced capped octahedral geometry and the central Mn^{III} atom five-coordinate ligated by four oxygen atoms of carbohydrate residues and one water molecule resulting in a square pyramidal geometry [70]. The $[\text{Mn}^{\text{II}}\text{Mn}^{\text{III}}\text{Mn}^{\text{II}}(\text{sal})_2(\text{Hsal})_2(\text{H}_2\text{O})_4(4\text{-Mepy})_6]^+$ cation is also composed of a linear trinuclear $\text{Mn}^{\text{II}}\text{Mn}^{\text{III}}\text{Mn}^{\text{II}}$ unit with the terminal Mn^{II} and the central Mn^{III} atoms in an octahedral environment [69].

The VI/V/VI compounds are essentially linear trimers comprising three edge-shared tetrahedra. The central Mn^{V} atom lies on a 2-fold axis of symmetry while the terminal imide ligands give $\text{Mn}-\text{N}$ distances in the range 1.554–1.674 Å, the imido bridges are strongly unsymmetrical with $\text{Mn}-\text{N}$ distances to the outer manganese averaging 1.87 and to the inner 1.77 Å and the $\text{Mn}-\text{Mn}$ distances lie in the range 2.463–2.490 Å [71].

3.1.2. Magnetic properties

The majority of the mixed-valence $\text{Mn}^{\text{III}}\text{Mn}^{\text{II}}\text{Mn}^{\text{III}}$ trinuclear compounds studied until now show a weak antiferromagnetic coupling with $S = 3/2$ ground states, J_{12} coupling varying from -3 to -7 cm^{-1} , $J_{11'} = 0$, $g_1 = 2.04$ and g_2 fixed at 2. Recently, three compounds showing a ferromagnetic behavior have been reported [66] (Table 3).

The susceptibility data for the $\alpha\text{-Mn}^{\text{III}}\text{Mn}^{\text{II}}\text{Mn}^{\text{III}}(\text{saladhp})_2(\text{OAc})_4(\text{CH}_3\text{OH})_2$ can be fitted to a model with a terminal Mn^{III} ion antiferromagnetically coupled to an $\text{Mn}^{\text{II/III}}$ spin system. The J coupling constant is -7.1 cm^{-1} indicating that the manganese atoms are weakly antiferromagnetically coupled in this complex. The water exchanged complex $\alpha\text{-Mn}^{\text{III}}\text{Mn}^{\text{II}}\text{Mn}^{\text{III}}(\text{Hsaladhp})_2(\text{OAc})_4(\text{H}_2\text{O})_2$ shows an identical r.t. solid-state moment ($\mu_{\text{eff}} = 8.1\text{ BM}$) and variable temperature susceptibility curve. Therefore, even though there are significant changes in the $\text{Mn}-\text{Mn}$ distance, the magnitude of the exchange coupling and the electronic ground state are unaltered. As a result of the obvious angular change, α and β forms of $\text{Mn}^{\text{III}}\text{Mn}^{\text{II}}\text{Mn}^{\text{III}}(\text{Hsaladhp})_2(\text{OAc})_4(\text{CH}_3\text{OH})_2$ exhibit different terminal manganese separations (6.5 and 7.1 Å, respectively) but it appears to have little consequence for the magnetic properties (α -isomer: $J = -7.1$; β -isomer: $J = -6.7\text{ cm}^{-1}$).

A more detailed analysis of the magnetic data is given for $\text{Mn}^{\text{III}}\text{Mn}^{\text{II}}\text{Mn}^{\text{III}}(\text{Hsaladhp})_2(\text{OAc})_2(5\text{-Cl-Hsal})_2(\text{thf})_2$. The value of μ_{eff} decreases from $7.94\text{ }\mu_{\text{B}}$ at 300 K to $3.4\text{ }\mu_{\text{B}}$ at 4 K. The $\mu_{\text{eff}}/3\text{Mn}$ at r.t. indicates the presence of a small antiferromagnetic interaction between the manganese atoms (spin-only value of 2Mn^{III} and Mn^{II} is $9.1\text{ }\mu_{\text{B}}$).

By virtue of crystallographic criteria the isotropic Heisenberg Hamiltonian for this complex is given by the following:

$$H = -2J_1(S_1S_2 + S_2S_3) - 2J_2(S_1S_3) \text{ where } S_1 = S_3 = 2 \text{ and } S_2 = 5/2$$

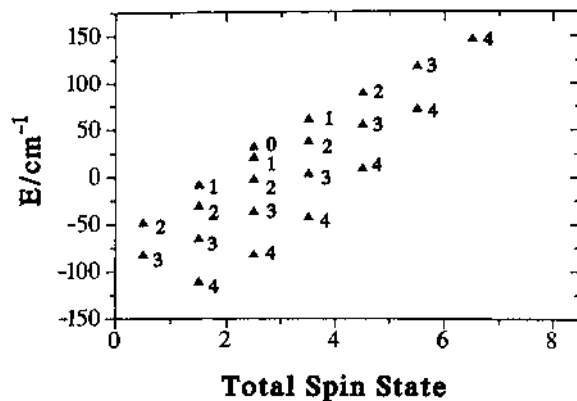


Fig. 8. Spin levels for $\text{Mn}^{\text{III}}\text{Mn}^{\text{II}}\text{Mn}^{\text{III}}(\text{Hsaladhp})_2(\text{OAc})_2(5\text{-Cl-Hsal})_2(\text{thf})_2$. The energy (in cm^{-1}) is given as a function of the spin value.

Because of the large distance between the terminal Mn^{III} ions (7.014 Å) we can exclude this interaction and, therefore, the major exchange interaction is expected between the terminal Mn^{III} and the central Mn^{II} . The exchange energies may be calculated by Kambe's method, and are given by the following:

$$E(S, S_{13}) = -J_1[S_T(S_T + 1) - S_{13}(S_{13} + 1) - S_2(S_2 + 1)]$$

Assuming isotropic g -values, the Zeeman term was added to the preceding Hamiltonian,

$$H_{\text{Zeeman}} = g\mu_B(S_1 + S_2 + S_3)B$$

Because of the extended hydrogen network, a mean field correction was added and the final expression of the susceptibility is given by the following:

$$\chi_{\text{MFC}} = \frac{\chi_{\text{M}}}{1 - \frac{2zJ\chi_{\text{M}}}{N\mu_B^2g^2}} \quad (4)$$

where

$$\chi_{\text{M}} = (Ng^2\mu_B^2/3\kappa T) \frac{\left[\sum_i S_i(S_i + 1)(2S_i + 1) \exp(-E_i/\kappa T) \right]}{\left[\sum_i (2S_i + 1) \exp(-E_i/\kappa T) \right]} \quad (5)$$

The magnetic parameters obtained from the fitting procedure are $J_1 = -5.6 \text{ cm}^{-1}$, $g = 1.95$ and $zJ = -0.25 \text{ cm}^{-1}$. Energy levels are represented in Fig. 8 with the addition of an S_{13} label. The ground state is found to be $|S_2 = 5/2, S_{13} = 4, S = 3/2\rangle$. This clearly shows that the lowest lying state is the $S = 3/2$ with reasonable population of a state, or states, of lower spin. For the $[\text{Mn}^{\text{II}}\text{Mn}^{\text{III}}\text{Mn}^{\text{II}}(\text{sal})_2(\text{Hsal})_2(\text{H}_2\text{O})_4(4\text{-Me-py})_6]^+$ cation, the magnetic data show an

antiferromagnetic behavior with $J = -0.53 \text{ cm}^{-1}$ and $D = -3.50 \text{ cm}^{-1}$, assuming $g = 2$, while the rhombic splitting parameter E can be neglected [69].

3.1.3. EPR study

All mixed-valence $\text{Mn}^{\text{III}}\text{Mn}^{\text{II}}\text{Mn}^{\text{III}}$ complexes are EPR active, while the $\text{Mn}^{\text{II}}\text{Mn}^{\text{III}}\text{Mn}^{\text{II}}$ and $\text{Mn}^{\text{VI}}\text{Mn}^{\text{V}}\text{Mn}^{\text{VI}}$ [71] compounds are EPR silent (as expected due to an even total electron number).

EPR spectra of trinuclear $\text{Mn}^{\text{III}}\text{Mn}^{\text{II}}\text{Mn}^{\text{III}}$ complexes with only acetates bridges, in CH_2Cl_2 , show a broad, low-field component which arises from the ground state spin quartet. A classic six-line spectrum from uncomplexed Mn^{II} is seen in MeOH due to dissociation to form monomeric units of Mn^{II} and $[\text{Mn}^{\text{III}}(\text{saladhp})]^+$. In dmf, a broad, low-field component for the trinuclear complex, the sharp six-line of the uncomplexed Mn^{II} and a multiline component centered at $g = 2$ with approximately 19 lines spread over 1900 G appear.

The powder EPR spectra of $\text{Mn}^{\text{III}}\text{Mn}^{\text{II}}\text{Mn}^{\text{III}}(\text{Hsaladhp})_2(\text{OAc})_2(5\text{-Cl-Hsal})_2(\text{thf})_2$ at 4 K exhibits a broad low-field signal at $g = 4.8$ indicating an $S = 3/2$ ground state (Fig. 9). It also exhibits a shoulder at $g = 6.7$ which is an indication of an admixture with the excited state $S = 5/2$ and a signal at $g = 2.0$ with poor intensity. The signal at the low-field region increases steadily until $T = 30 \text{ K}$.

At r.t. a new signal at $g = 9.7$ appears with a weak feature at $g = 4.3$ and $g = 2.0$. Because all the states are populated at r.t. it is quite difficult to indicate the origin

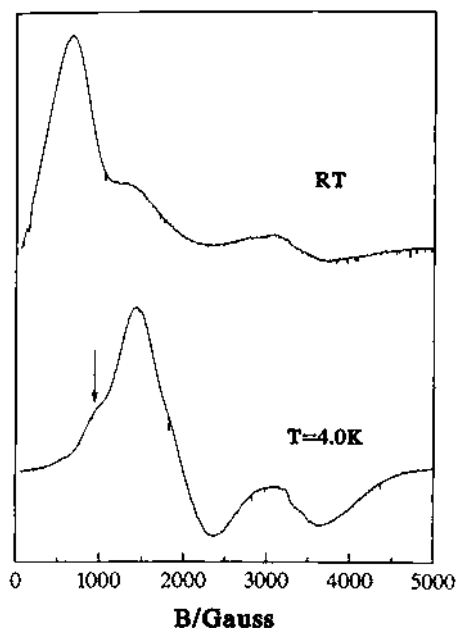


Fig. 9. X-band powder EPR spectra of $\text{Mn}^{\text{III}}\text{Mn}^{\text{II}}\text{Mn}^{\text{III}}(\text{Hsaladhp})_2(\text{OAc})_2(5\text{-Cl-Hsal})_2(\text{thf})_2$ at r.t. and at 4 K.

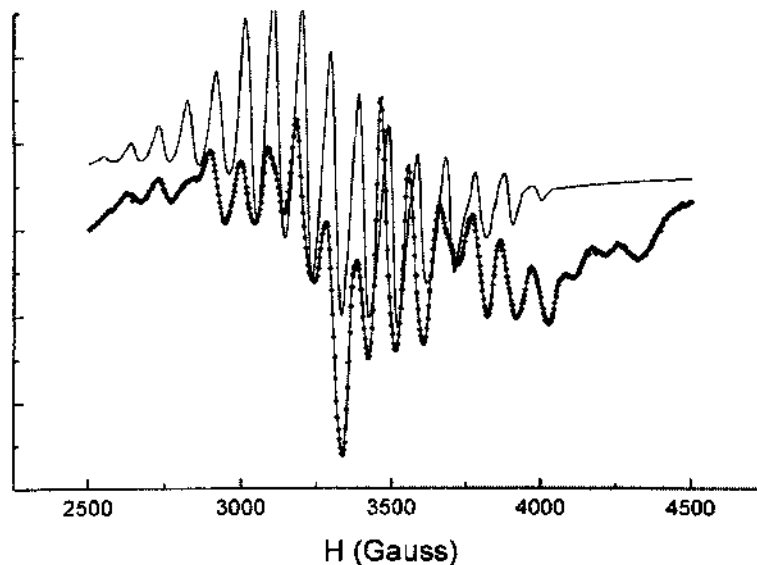


Fig. 10. EPR spectra of $\text{Mn}^{\text{III}}\text{Mn}^{\text{II}}\text{Mn}^{\text{III}}(5\text{-Cl-Hsaladhp})_2(\text{Sal})_4$ in CHCl_3 . Dot-line: the recorded EPR spectrum; solid-line: the simulated EPR spectrum.

of this new signal. Temperature-dependent population interconversion has been suggested as the origin of the two S_2 state EPR spectral signatures.

In CH_2Cl_2 glass a very broad signal centered at $g = 4.3$ appears which strongly indicates an $S = 3/2$ state, while a signal at $g = 2.0$ with more than six lines is observed. The temperature dependence of the EPR spectrum reveals that both signals come from the same compound as the intensity of the signals at $g = 4.3$ and $g = 2$ decrease when the temperature is decreased. In addition, hyperfine structure is observed in the $g = 4.3$ signal.

The EPR spectrum for $\text{Mn}^{\text{III}}\text{Mn}^{\text{II}}\text{Mn}^{\text{III}}(5\text{-Cl-Hsaladhp})_2(\text{Sal})_4$ was obtained at 4 K in CHCl_3 glass (Fig. 10). The low-field EPR region shows a superposition of two signals, one centered around $g = 3.6$ and the other, with hyperfine structure, centered around $g = 4.1$ (indicating an $S = 3/2$ state); a 19-line signal at $g = 2.0$ is also observed. The hyperfine structure in the $g = 4.1$ signal is consistent with previous reports [60,61]. The observed EPR spectrum is assigned to the trinuclear compound, as there is no dissociation of this complex in CHCl_3 . The simulation of the multiline signal at $g \approx 2$ was carried out in the strong exchange approximation, considering only $\Delta M_s = 1$, $\Delta M_l = 0$ transitions [65]. The simulation parameters are: $g_{\parallel} = 1.97$, $g_{\perp} = 2.02$, $A_{\parallel}\text{Mn}^{\text{II}} = 110 \times 10^{-4} \text{ cm}^{-1}$, $A_{\perp}\text{Mn}^{\text{II}} = 88 \times 10^{-4} \text{ cm}^{-1}$, $A_{\parallel}\text{Mn}^{\text{III}} = 51 \times 10^{-4} \text{ cm}^{-1}$, $A_{\perp}\text{Mn}^{\text{III}} = 91 \times 10^{-4} \text{ cm}^{-1}$, $\sigma = 22 \text{ G}$. Zeeman g factors refer to the molecule and hyperfine A factors refer to the interaction between the total electronic spin and the individual nuclear spins. A Lorentzian line shape was used with the same linewidth for all transitions. The $g = 2$ multiline signal of the S_2 oxidation state of the water-oxidation manganese center has

provided the basis for much speculation as to the nuclearity and oxidation states of the manganese ions in the OEC.

Mixed-valence dimers, such as $\text{Mn}^{\text{III}}\text{Mn}^{\text{II}}$ or $\text{Mn}^{\text{III}}\text{Mn}^{\text{IV}}$, and tetranuclear $\text{Mn}^{\text{III}}\text{Mn}^{\text{III}}\text{Mn}^{\text{III}}\text{Mn}^{\text{IV}}$ compounds exhibit multiline features. A recent theoretical approach [72] concludes that a tetranuclear cluster is responsible for the EPR signal and that the hyperfine couplings must be anisotropic [73]. This study [72] also suggests that the Mn^{III} ion(s) may be five-coordinate, having distorted trigonal bipyramidal geometry with an $(e')^2(e'')^2$ configuration. A possible explanation given as to why there could be five-coordinate Mn^{III} ions in the S_2 state of the OEC is that one or both of the substrate water molecules may not be bound (yet) to manganese cluster. Therefore, the presence of five-coordinate Mn atoms in $\text{Mn}^{\text{III}}\text{Mn}^{\text{II}}\text{Mn}^{\text{III}}(\text{5-Cl-Hsaladhp})_2(\text{Sal})_4$ could provide an interesting case for studying the effects the coordination of water on the spectroscopic and structural features of such clusters.

In summary, among the known Mn clusters, the compound reported here exhibits the unique feature of possessing a 19-line EPR signal similar to that of the OEC in the S_2 or S^* states. While EPR spectroscopy cannot be used as a structural tool to resolve complicated problems of this type, it is nevertheless interesting that the multiline signal of OEC has not been reproduced by any Mn complex so far. Unfortunately, a $[\text{Mn}_4]$ model satisfying the number of lines, the line shapes and widths and anisotropic hyperfine coupling and five-coordinate Mn^{III} ion has not yet appeared in the literature. It is remarkable that the structure presented in this report, while not a tetranuclear complex, satisfies all the of above characteristics, and thus could be considered relevant to the trimer/monomer model, which is one of those proposed for the OEC [1,74,75] (Fig. 11).

3.2. Close-structure mixed-valence trinuclear $\text{Mn}^{\text{III}}\text{Mn}^{\text{II}}\text{Mn}^{\text{III}}$ complexes

Trinuclear $\text{Mn}^{\text{III}}\text{Mn}^{\text{II}}\text{Mn}^{\text{III}}$ complexes possess the ‘basic carboxylate’ structure having a Mn_3O core (Fig. 12) with the Mn_3 occupying an equilateral or an isosceles triangle depending on the valence situation.

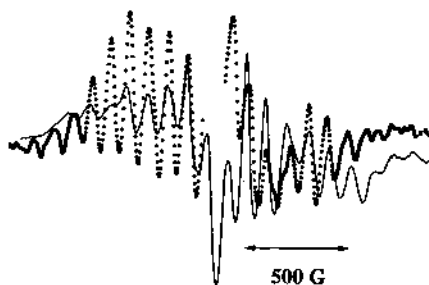


Fig. 11. Solid-line: EPR spectrum of $\text{Mn}^{\text{III}}\text{Mn}^{\text{II}}\text{Mn}^{\text{III}}(\text{5-Cl-Hsaladhp})_2(\text{Sal})_4$ in CHCl_3 ; dot-line: the EPR spectrum of S_2 state of OEC.

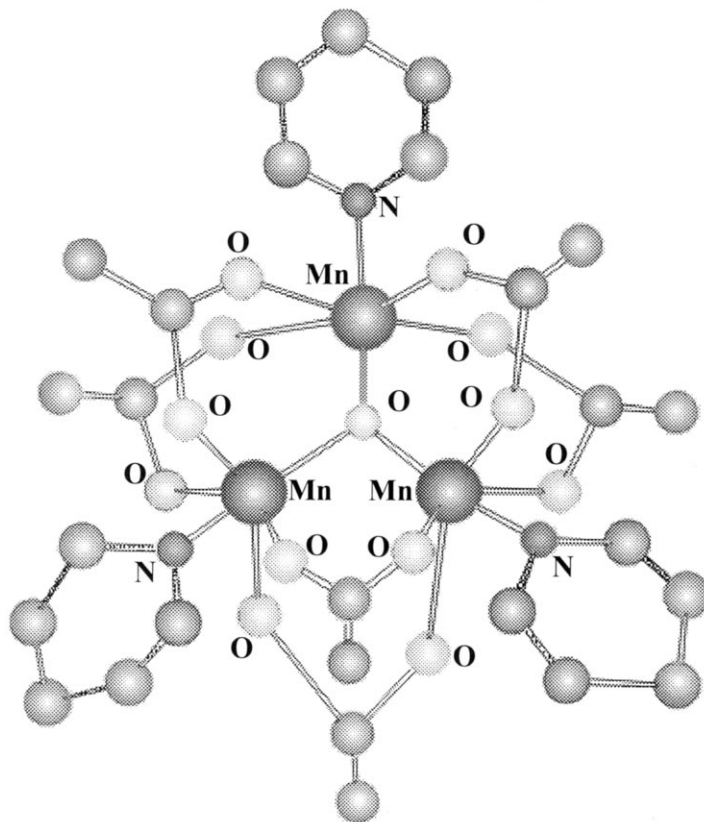


Fig. 12. The crystal structure of $\text{Mn}^{\text{III}}\text{Mn}^{\text{II}}\text{Mn}^{\text{III}}\text{O}(\text{OAc})_6(\text{py})_3$ showing the Mn_3O core.

Valence-trapped complexes with $\text{Mn}^{\text{II}}\text{--O}$ distances distinguish longer than the $\text{Mn}^{\text{III}}\text{--O}$ distances lead to isosceles rather than equilateral Mn_3 triangle. In the latter case the $\text{Mn}^{\text{III}}\cdots\text{Mn}^{\text{III}}$ distances (3.214–3.285 Å) are significantly shorter than the $\text{Mn}^{\text{II}}\cdots\text{Mn}^{\text{III}}$ distances (3.350–3.418 Å). The average $\text{Mn}\cdots\text{Mn}$ separation (3.330 Å), however, is quite similar to that seen in the electronically delocalized complexes (3.353–3.363 Å) (Table 5). All the mixed-valence $\text{Mn}^{\text{III}}\text{Mn}^{\text{II}}\text{Mn}^{\text{III}}$ trinuclear compounds studied until now show a weak antiferromagnetic coupling with $S = 3/2$ or $1/2$ ground states, J coupling characterizing the $\text{Mn}^{\text{II}}\cdots\text{Mn}^{\text{III}}$ interaction and J^* the $\text{Mn}^{\text{III}}\cdots\text{Mn}^{\text{III}}$ interaction, varying from -5.2 to -6.5 cm^{-1} and from -2.7 to -4.5 cm^{-1} , respectively.

The EPR spectra of $[\text{Mn}^{\text{III}}\text{Mn}^{\text{II}}\text{Mn}^{\text{III}}\text{O}(\text{OAc})_6(\text{py})_3](\text{py})$ at 2 K show a strong signal in the $g = 4$ region revealing that the spin ground state is $3/2$. The intensity of this signal decreases with increasing temperature, indicating a depopulation of this state as the temperature is increased. The temperature dependence is consistent with the lowest energy state being the $\pm 1/2$ Kramers doublet from the $S = 3/2$ state which should give rise to two EPR transitions with $g_{\parallel} \sim 2$ and $g_{\perp} \sim 4$ [81].

Table 5
Close-structure trinuclear $\text{Mn}^{\text{III}}\text{Mn}^{\text{II}}\text{Mn}^{\text{III}}$ complexes

Formula	Mn...Mn separation (Å)	J (cm^{-1})	J^* (cm^{-1})	g	S	Ref.
$[\text{Mn}^{\text{III}}\text{Mn}^{\text{II}}\text{Mn}^{\text{III}}\text{O}(\text{OAc})_6(\text{py})_3](\text{py})$	3.363	–5.2	–2.7	2.05	3/2	[82–84]
$\text{Mn}^{\text{III}}\text{Mn}^{\text{II}}\text{Mn}^{\text{III}}\text{O}(\text{OAc})_6(3\text{-ClC}_5\text{H}_4\text{N})_3$	–	Antiferromagnetic	–	–	–	[85]
$\text{Mn}^{\text{III}}\text{Mn}^{\text{II}}\text{Mn}^{\text{III}}\text{O}(\text{O}_2\text{CPh})_6(\text{py})_2(\text{H}_2\text{O}) \cdot 0.5\text{CH}_3\text{CN}$	3.218, 3.418, 3.396	–6.5	–4.5	1.99	1/2	[82,83]
$[\text{Mn}^{\text{III}}\text{Mn}^{\text{II}}\text{Mn}^{\text{III}}\text{O}(\text{O}_2\text{CPh})_6(\text{py})_3] \cdot 2\text{CH}_3\text{CN}$	3.284, 3.285, 3.403	–	–	–	–	[87]

The EPR spectra for a polycrystalline sample of $\text{Mn}^{\text{III}}\text{Mn}^{\text{II}}\text{Mn}^{\text{III}}\text{O}(\text{O}_2\text{CPh})_6(\text{py})_2(\text{H}_2\text{O}) \cdot 0.5\text{CH}_3\text{CN}$ complex clearly show that the broad signal at $g \sim 1.78$ with a weak signal at $g \sim 4$ comes from $\pm 1/2$ Kramers doublet of $S = 1/2$ ground state [81,85]

Acknowledgements

The author's special thanks goes to the collaborators whose work has been summarized in this article, Prof. V.L. Pecoraro and his group (University of Michigan), D.A. Malamataris, P. Hitou, V. Stergiou, G. Psomas, Dr Dendrinou-Samara (University of Thessaloniki), Prof. T.A. Kabanos, K. Soulti (University of Ioannina), Dr A. Terzis, Dr C.P. Raptopoulou, Dr V. Tangoulis, A. Tsochos (CNR 'Demokritos').

References

- [1] V.L. Pecoraro (Ed.), Manganese Redox Enzymes, VCH, New York, 1992.
- [2] J. Stube, J. Biol. Chem. 265 (1990) 5329.
- [3] J.B. Lynch, C. Juarez-Garcia, E. Munck, L. Que Jr., J. Biol. Chem. 264 (1989) 8091.
- [4] P. Nordlund, B.-M. Sjöberg, H. Eklund, Nature 345 (1990) 593.
- [5] M. Atta, P. Nordlund, A. Aberg, H. Eklund, M. Fontecave, J. Biol. Chem. 267 (1992) 682.
- [6] R. Cammack, A. Chapman, L. Wei-Ping, A. Katagouni, D.P. Kelly, FEBS Lett. 253 (1989) 239.
- [7] M.L. Ludwig, A.L. Metzger, K.A. Patridge, W.C. Stallings, J. Mol. Biol. 219 (1991) 335.
- [8] H. Wariishi, M.H. Gold, J. Biol. Chem. 265 (1990) 2070.
- [9] H. Wariishi, H.B. Dunford, I.D. MacDonald, M.H. Gold, J. Biol. Chem. 264 (1989) 3335.
- [10] Y. Kono, I. Fridovich, J. Biol. Chem. 258 (1983) 13646.
- [11] G.S. Waldo, R.M. Fronko, J.E. Penner-Hahn, Biochemistry 30 (1991) 10486.
- [12] R.M. Fronko, J.E. Penner-Hahn, C.J. Bender, J. Am. Chem. Soc. 110 (1988) 7554.
- [13] D.R. Gamelin, M.L. Kirk, T.L. Stemmler, S. Pal, W.H. Armstrong, J.E. Penner-Hahn, E.I. Solomon, J. Am. Chem. Soc. 116 (1994) 2392.
- [14] J. Messinger, J.H.A. Nugent, M.C.W. Evans, Biochemistry 36 (1997) 11055.
- [15] G.M. Ananyev, G.C. Dismukes, Biochemistry 35 (1996) 4102.
- [16] V.K. Yachandra, K. Sauer, M.P. Klein, Chem. Rev. 96 (1996) 2927.
- [17] R.J. Debus, Biochim. Biophys. Acta 1102 (1992) 269.
- [18] A.W. Rutherford, J.-L. Zimmermann, A. Boussac, in: J. Barber (Ed.), Photosystems: Structure, Function and Molecular Biology, Elsevier, Amsterdam, 1992, p. 179.
- [19] T.-A. Ono, T. Noguchi, Y. Inoue, M. Kusunoki, T. Matsushita, H. Oyanagi, Science 258 (1992) 1335.
- [20] N.Y. Chirgadze, I.P. Kuranova, N.A. Nevskaya, A.V. Teplyakov, K. Wilson, B.V. Srokopytov, E.G. Harutyunyan, W. Hohne, Kristallografiya 36 (1991) 128.
- [21] R.L. Rardin, A. Bino, P. Poganiuch, W.B. Tolman, S. Liu, S.J. Lippard, Angew. Chem. Int. Ed. Engl. 29 (1990) 812.
- [22] S. Menage, S.E. Vitols, P. Bergerat, E. Codjovi, O. Kahn, J.-J. Girerd, M. Guillot, X. Solans, T. Calvet, Inorg. Chem. 30 (1991) 2666.
- [23] R.L. Rardin, P. Poganiuch, A. Bino, D.P. Goldberg, W.B. Tolman, S. Liu, S.J. Lippard, J. Am. Chem. Soc. 114 (1992) 5240.
- [24] V. Tangoulis, D.A. Malamataris, K. Soulti, V. Stergiou, C.P. Raptopoulou, A. Terzis, T.A. Kabanos, D.P. Kessissoglou, Inorg. Chem. 35 (1996) 4974.

- [25] C.H.L. Kennard, G. Smith, E.J. O' Reilly, W. Chiangjin, *Inorg. Chim. Acta* 69 (1983) 53.
- [26] T. Lis, *Acta Crystallogr.* B33 (1977) 2964.
- [27] (a) K. Hubner, H.W. Roesky, M. Noltemeyer, R. Bohra, *Chem. Ber.* 124 (1991) 515. (b) Z.J. Zhong, X.-Z. You, *Polyhedron* 13 (1994) 2157.
- [28] E.F. Bertaut, T.Q. Duc, P. Burlet, M. Thomas, J.M. Moreau, *Acta Crystallogr.* B30 (1974) 2234.
- [29] M. Osawa, U.P. Singh, M. Tanaka, Y. Moro-oka, N. Kitajima, *J. Chem. Soc. Chem. Commun.* (1993) 310.
- [30] T. Lis, B. Jezowska-Trzebiatowska, *Acta Crystallogr.* B33 (1977) 2112.
- [31] K. Wieghardt, U. Bossek, B. Nuber, J. Weiss, J. Bonvoisin, M. Corbella, S.E. Vitols, J.-J. Girerd, *J. Am. Chem. Soc.* 110 (1988) 7398.
- [32] U. Bossek, K. Wieghardt, B. Nuber, J. Weiss, *Inorg. Chim. Acta* 165 (1989) 123.
- [33] X.-M. Chen, T.C.W. Mak, *Inorg. Chim. Acta* 189 (1991) L3.
- [34] H. Oshio, E. Ino, I. Mogi, T. Ito, *Inorg. Chem.* 32 (1993) 5697.
- [35] J. Cano, G.D. Munno, J. Sanz, R. Ruiz, F. Lloret, J. Faus, M. Julve, *J. Chem. Soc. Dalton Trans.* (1994) 3465.
- [36] V. Tangoulis, G. Psomas, C. Dendrinou-Samara, C.P. Raptopoulou, A. Terzis, D.P. Kessissoglou, *Inorg. Chem.* 35 (1996) 7655.
- [37] X.-M. Chen, Y.-X. Tong, Z.-T. Xu, T.C.W. Mak, *J. Chem. Soc. Dalton Trans.* (1995) 4001.
- [38] A. Karipidis, A.T. Reed, *Inorg. Chem.* 15 (1976) 44.
- [39] T. Tanase, S.J. Lippard, *Inorg. Chem.* 34 (1995) 4682.
- [40] Y. Gultneh, A. Farooq, S. Liu, K.D. Karlin, J. Zubieta, *Inorg. Chem.* 31 (1992) 3607.
- [41] S.-B. Yu, S.J. Lippard, I. Shweky, A. Bino, *Inorg. Chem.* 31 (1992) 3502.
- [42] R.A. Reynolds, W.O. Yu, W.R. Dunham, D. Coucouvanis, *Inorg. Chem.* 35 (1996) 2721.
- [43] R.D. Cannon, R.P. White, *Prog. Inorg. Chem.* 36 (1988) 195.
- [44] S.L. Dexheimer, M.P. Klein, *J. Am. Chem. Soc.* 114 (1992) 2821.
- [45] D. Koulougliotis, D.J. Hirsh, G.W. Brudvig, *J. Am. Chem. Soc.* 114 (1992) 8322.
- [46] G.C. Dismukes, Y. Siderer, *FEBS Lett.* 121 (1980) 78.
- [47] G.W. Brudvig, J.L. Casey, K. Sauer, *Biochim. Biophys. Acta* 723 (1983) 366.
- [48] J.-L. Zimmerman, A.W. Rutherford, *Biochim. Biophys. Acta* 767 (1984) 160.
- [49] O. Hansson, R. Aasa, T. Vaenngaard, *Biophys. J.* 51 (1987) 825.
- [50] J. Cole, V.K. Yachandra, R.D. Guiles, A.E. McDermott, R.D. Britt, S.L. Dexheimer, K. Sauer, M.P. Klein, *Biochim. Biophys. Acta* 890 (1987) 395.
- [51] J. Messinger, J.H.A. Nugent, M.C.W. Evans, *Biochemistry* 36 (1997) 11055.
- [52] J.E. Penner-Hahn, R.M. Fronko, V.L. Pecoraro, C.F. Yocum, S.D. Betts, N.R. Bowlby, *J. Am. Chem. Soc.* 112 (1990) 2549.
- [53] V.L. Pecoraro, M.J. Baldwin, A. Gelasco, *Chem. Rev.* 94 (1994) 807.
- [54] W. Liang, M.J. Latimer, H. Dau, T.A. Roelofs, V.K. Yachandra, K. Sauer, M.P. Klein, *Biochemistry* 33 (1994) 4923.
- [55] R.D. Guiles, V.K. Yachandra, A.E. McDermott, J.L. Cole, S.L. Dexheimer, R.D. Britt, K. Sauer, M.P. Klein, *Biochemistry* 29 (1990) 486.
- [56] P.J. Riggs-Gelasco, R. Mei, C.F. Yocum, J.E. Penner-Hahn, *J. Am. Chem. Soc.* 118 (1996) 2387.
- [57] H. Dau, J.C. Andrews, T.A. Roelofs, M.J. Latimer, W. Liang, V.K. Yachandra, K. Sauer, M.P. Klein, *Biochemistry* 34 (1995) 5274.
- [58] X.-h. Li, D.P. Kessissoglou, M.L. Kirk, C. Bender, V.L. Pecoraro, *Inorg. Chem.* 27 (1988) 1.
- [59] D.P. Kessissoglou, M.L. Kirk, C.A. Bender, M.S. Lah, V.L. Pecoraro, *J. Chem. Soc. Chem. Commun.* (1989) 84.
- [60] D.P. Kessissoglou, M.L. Kirk, M.S. Lah, X.-h. Li, C.A. Raptopoulou, W.E. Hatfield, V.L. Pecoraro, *Inorg. Chem.* 31 (1992) 5424.
- [61] D.A. Malamatari, P. Hitou, A.G. Hatzidimitriou, F.E. Inscore, A. Gourdon, M.L. Kirk, D.P. Kessissoglou, *Inorg. Chem.* 34 (1995) 2493.
- [62] D.P. Kessissoglou, W.M. Butler, V.L. Pecoraro, *J. Chem. Soc. Chem. Commun.* (1986) 1253.
- [63] D.P. Kessissoglou, X.-h. Li, W.M. Butler, V.L. Pecoraro, *Inorg. Chem.* 26 (1987) 2487.
- [64] D.P. Kessissoglou (Ed.), *Bioinorganic Chemistry: An Inorganic Perspective of Life*, Kluwer, Dordrecht, 1994, p. 299.

- [65] V. Tangoulis, D.A. Malamataris, A. Tsochos, C.P. Raptopoulou, A. Terzis, D.P. Kessissoglou, in preparation.
- [66] M. Hirotsu, M. Kojima, Y. Yoshikawa, *Bull. Chem. Soc. Jpn.* 70 (1997) 649.
- [67] S. Shoner, P. Power, *Inorg. Chem.* 31 (1992) 1001.
- [68] Y.-G. Wei, S.-W. Zhang, M.-C. Shao, Q. Liu, Y.-O. Tang, *Polyhedron* 15 (1996) 4303.
- [69] X.S. Tan, J. Sun, C.H. Hu, D.G. Fu, D.F. Xiang, P.J. Zheng, W.X. Tang, *Inorg. Chim. Acta* 257 (1997) 203.
- [70] S. Yano, M. Doi, S. Tamakoshi, W. Mori, M. Mikuriya, A. Ichimura, I. Kinoshita, Y. Yamamoto, T. Tanase, *J. Chem. Soc. Chem. Commun.* (1997) 997.
- [71] A.A. Danopoulos, G. Wilkinson, T.K.N. Sweet, M.B. Hursthouse, *J. Chem. Soc. Dalton Trans.* (1995) 937.
- [72] M. Zheng, G.C. Dismukes, *Inorg. Chem.* 35 (1996) 3307.
- [73] D.H. Kim, R.D. Britt, M.P. Klein, K. Sauer, *Biochemistry* 31 (1992) 541.
- [74] V.L. Pecoraro, D.P. Kessissoglou, X.-h. Li, M.S. Lah, S. Saadeh, C.A. Bender, J.A. Bonadies, E. Larson, *Curr. Res. Photosynth. I* (1990) 709.
- [75] R.J. Debus, *Biochem. Biophys. Acta* 1102 (1992) 269.
- [76] S. Pal, M.K. Chan, W.H. Armstrong, *J. Am. Chem. Soc.* 114 (1992) 6398.
- [77] S. Pal, W.H. Armstrong, *Inorg. Chem.* 31 (1992) 5417.
- [78] K.R. Reddy, M.V. Rajasekharan, N. Arulsamy, D.J. Hodgson, *Inorg. Chem.* 35 (1996) 2283.
- [79] N. Auger, J.-J. Girerd, M. Corbella, A. Gleizes, J.-L. Zimmerman, *J. Am. Chem. Soc.* 112 (1990) 448.
- [80] J.E. Sarneski, H.H. Thorp, G.W. Brudvig, R.H. Crabtree, G.K. Schutle, *J. Am. Chem. Soc.* 112 (1990) 7255.
- [81] J.K. McCusker, H.G. Jang, S. Wang, G. Christou, D.N. Hendrickson, *Inorg. Chem.* 31 (1992) 1874.
- [82] J.B. Vincent, H.-R. Chang, K. Folting, J.C. Huffman, G. Christou, D.N. Hendrickson, *J. Am. Chem. Soc.* 109 (1987) 5703.
- [83] A.R.E. Baikie, M.B. Hursthouse, D.B. New, P. Thornton, *J. Chem. Soc. Chem. Commun.* (1978) 62.
- [84] A.R.E. Baikie, M.B. Hursthouse, D.B. New, P. Thornton, R.G. White, *J. Chem. Soc. Chem. Commun.* (1980) 684.
- [85] S.M. Oh, D.N. Hendrickson, K.L. Hasset, R.E. Davis, *J. Am. Chem. Soc.* 107 (1985) 8009.
- [86] Z.J. Zhong, J.-Q. Tao, H. Li, X.-Z. You, T.C.W. Mak, *Polyhedron* 16 (1997) 1719.